Progress In Electromagnetics Research C, Vol. 138, 51–63, 2023

Multiband Patch Antenna with SINC-Shaped Edges for Sub-6 GHz Applications

Qusai H. Sultan[1], Ahmed M. A. Sabaawi[1, *], Bariq M. Abawi[2], and Saad W. O. Luhaib[3]

Abstract—In this paper, several multiband patch antennas with sinc-shaped edges were analyzed, designed, simulated, and implemented for modern sub-6 GHz applications. The aim is to use the sinc function parameters such as amplitude and number of maxima (frequency) to control the antenna performance such as resonance and radiation characteristics. It is shown that changing the sinc pattern parameters has a significant impact on the resonance of the antenna, and hence these parameters can be used to directly control the multiband behavior of the antenna. The proposed antenna designs were manufactured, and their performance was tested experimentally in the lab and compared to simulation results. An acceptable agreement between experimental and simulated results was achieved.

1. INTRODUCTION

The advent of fifth-generation (5G) wireless communication systems has brought about a typical shift in the domain of communication systems, promising surpassing data rates, low latency, and enhanced connectivity for a wide range of applications. The realization of the full potential of 5G relies on the development of efficient antennas capable of supporting the urgent requirements of this rapidly growing technology. Among the various antenna types, multiband patch antennas have emerged as a promising candidate to address the merged demands of 5G applications [1]. The increasing need for faster data rates and uninterrupted connectivity requires the investigation of inventive antenna designs that can function across various frequency bands to meet the growing requirements of 5G networks. Multiband patch antennas provide an effective solution to this issue, as they can be designed to operate at multiple frequencies, covering a wide range of the spectrum while remaining compact in size [2].

With the rapidly increasing demand for enhanced data capacity and uninterrupted connectivity, there is a need for innovative antenna designs that can efficiently function across various frequency bands. These antenna designs aim to effectively exploit most of the abundant spectrum resources available to 5G networks. Multiband patch antennas have demonstrated great potential in this regard by offering the advantage of resonating at multiple frequencies simultaneously. In addition, they maintain compact size and ease of integration into contemporary wireless devices.

Recent literature reflects the increasing interest and extensive research on multiband patch antennas for 5G applications. Researchers have demonstrated remarkable achievements in achieving multiband behavior by adopting various novel techniques and materials. For instance, metamaterial-inspired structures [3–6], frequency selective surfaces (FSS) [7–9], and advanced tuning methods have been employed to broaden the operating bandwidth and enhance the performance of these antennas [10–13]. Moreover, studies have shown that multiband patch antennas can significantly enhance the spectral efficiency and overall capacity of 5G networks [14–17]. By providing access to multiple frequency bands, these antennas enable a higher data rate and improved coverage, catering to the diverse needs

Received 1 August 2023, Accepted 17 September 2023, Scheduled 30 September 2023
* Corresponding author: Ahmed M. A. Sabaawi (ahmed.sabaawi@uoninevah.edu.iq).
[1] College of Electronics Engineering, Ninevah University, Mosul, Iraq. [2] College of Information Technology, Ninevah University, Mosul, Iraq. [3] College of Engineering, Mosul University, Mosul, Iraq.

of contemporary communication systems. Despite the significant advancements in multiband patch antenna design, there remain certain challenges and limitations that warrant further investigation. Mutual coupling effects, interference between different bands, and size constraints are some of the issues that researchers have been grappling with [18]. Addressing these challenges is crucial for the successful integration of multiband patch antennas into practical 5G devices and systems.

The objective of this research paper is to control the radiation and reflection characteristics of patch antenna by an organized process of altering its geometry. To this end, sinc function is incorporated at the edges of the antenna to control the resonant frequency of the antenna by changing the parameters of the function.

2. SINC-SHAPED EDGES OF RECTANGULAR PATCH ANTENNA

The width of the rectangular patch was integrated with a sinc-shape edges as shown in Fig. 1. In this design, the dimension of patch length along x-axis is varied as a sinc function with positive amplitude.

The equation of upper sinc part for the patch length at any value of x within the range of $-W/2 \leq x \leq W/2$ is given by:

$$L_{\text{sinc}}(x) = Amp. * \text{sinc}\ (\alpha x) \tag{1}$$

where:

$$\alpha = m = \frac{n\pi}{\frac{W}{2}} \tag{2}$$

And

$$x \in \left[-\frac{W}{2}, \frac{W}{2}\right] \tag{3}$$

$Amp.$ is the amplitude value of sinc function, and m is the frequency argument.

The total length of the patch will vary according to the value of (x) as follows:

$$L(x) = L_{edge} + 2 * L_{\text{sinc}}(x) \tag{4}$$

L_{edge} is the length of rectangular patch when $Amp. = 0$, which is approximately equal to half-length of wavelength for the first resonance frequency. This value can be calculated based on known equations to calculate the length of rectangular patch antenna.

$$L_{\text{sinc}}(x) = Amp. * \text{sinc}\ (mx) = \begin{cases} Amp. * \dfrac{\sin(mx)}{mx}, & x \neq 0 \\ Amp., & x = 0 \end{cases} \tag{5}$$

In the design shown in Fig. 1, the values of parameters are chosen as $Amp. = 9$ and $m = 1$.

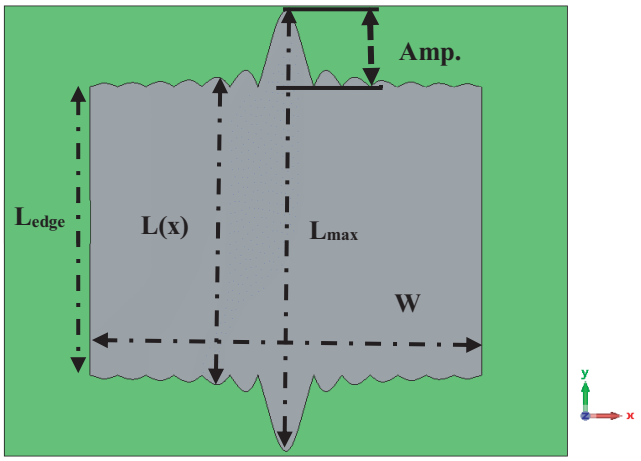

Figure 1. Rectangular patch antenna with sinc-shaped edges.

3. PARAMETRIC STUDY AND SIMULATION RESULTS

In order to check the impact of the sinc-shaped edges on the patch antenna performance, three rectangular patch antennas are designed and simulated. The first antenna is a conventional rectangular patch antenna with inset feeding (i.e., $Amp. = 0$), and the second one is a rectangular patch antenna with sinc-shaped edges that have positive sinc amplitude ($Amp. = 9$ and $m = 2$) while the third antenna is similar to the second one but with negative sinc amplitude ($Amp. = -9$ and $m = 2$). Fig. 2 illustrates the geometrical details of the three designed antennas.

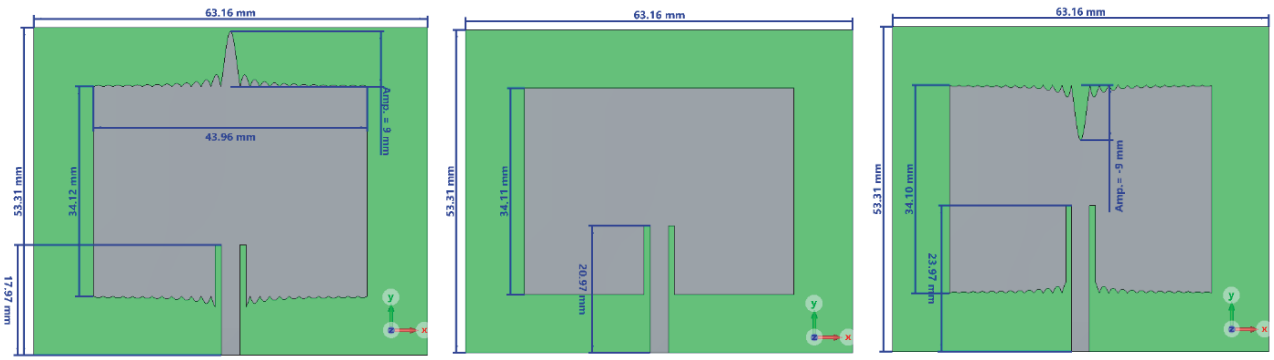

(a) (b) (c)

Figure 2. Rectangular patch antenna with sinc-shaped edges: (a) With positive amplitude sinc, (b) without sinc edge (i.e., $Amp. = 0$), and (c) with negative amplitude sinc.

CST Studio Suite is utilized to simulate the designed antennas in this work. The antenna is placed on an FR-4 substrate layer with $\varepsilon_r = 4.3$ and $h = 1.6$ mm. The simulated S-parameters of the designed antenna in Fig. 2 are shown in Fig. 3. It is clearly seen that employing the sinc function in the geometry of the antenna has a direct impact on the antenna resonant frequency. For the conventional rectangular patch, the antenna exhibits four bands resonance located in the sub-6 GHz at around 2.1 GHz, 3.3 GHz, 4 GHz, and 5.3 GHz. However, when the length of the patch was altered with a sinc-shaped edge that has a positive amplitude, the resonant frequency of all bands is reduced because the overall length of patch is increased (i.e., $L > \lambda/2$). On the other hand, the negative sinc function has caused an increment in the resonant frequency of the antenna at all bands because the overall length of patch is deceased (i.e., $L < \lambda/2$). Based on the evident impact of the sinc function on the antenna performance, it is expected that the resonant frequency can be tuned perfectly by varying the parameter of the sinc function such as $Amp.$, m and x. Thus, a parametric study will be conducted with an extensive simulations to achieve an optimum antenna performance for the 5G applications.

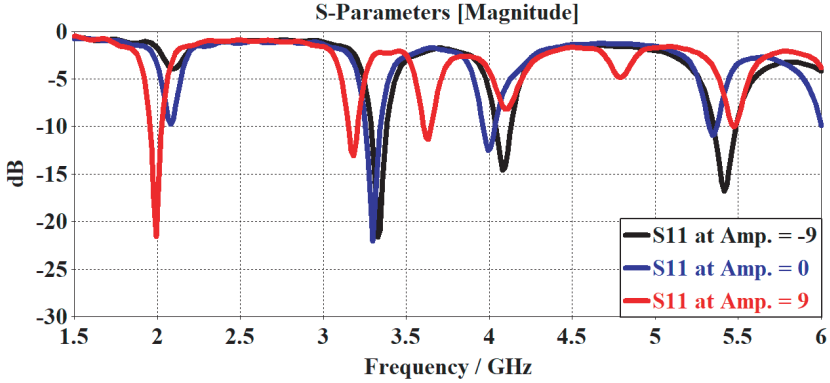

Figure 3. Simulated return loss (S_{11}) for the designed antennas at different values of $Amp.$ (in mm).

The sinc function parameters have been varied as follows: ($-9\,\text{mm} \leq Amp. \leq 9\,\text{mm}$) with step $= 3\,\text{mm}$ and ($0.5 \leq m \leq 2$) with step $= 0.5$. The total combination of varying the aforementioned sinc parameters simultaneously are around 35 cases. The S_{11} results of all combinations are shown in Fig. 4. It is found that increasing the amplitude will decrease the resonant frequency (shifted smoothly to the left). In contrast, increasing the value of (m) will increase the resonant frequency when the sinc amplitude is positive, and on the other hand, increasing the value of (m) will decrease the resonant frequency if the sinc amplitude is negative. Thus, by varying both $Amp.$ and m, we can control the resonant frequency of the antenna and frequency distance between bands, which gives the designer a degree of freedom in targeting a specific frequency band. This also helps in the process of fine tuning of antenna's resonance frequency.

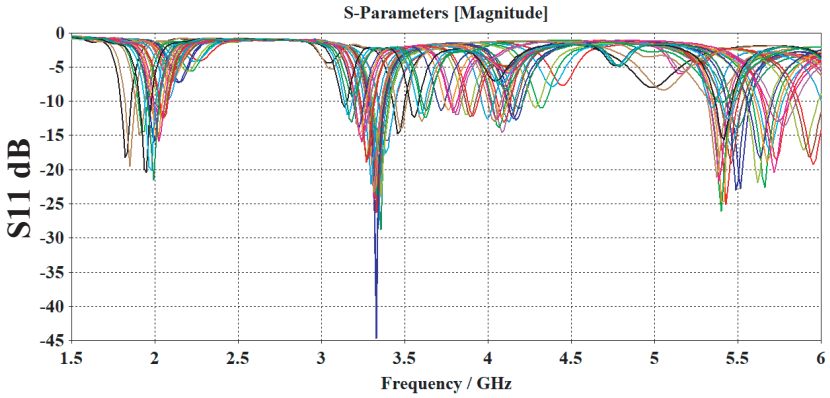

Figure 4. Simulated return loss (S_{11}) for all cases in the parametric study.

Out of all the above combinations, only four cases were selected to be adopted throughout this article. These cases are selected based on the number of bands, and the reflection coefficient that fits well with the 5G applications. Fig. 5 depicts the simulated S_{11} of the selected antennas. The geometrical details of the four selected antennas are illustrated in Fig. 6.

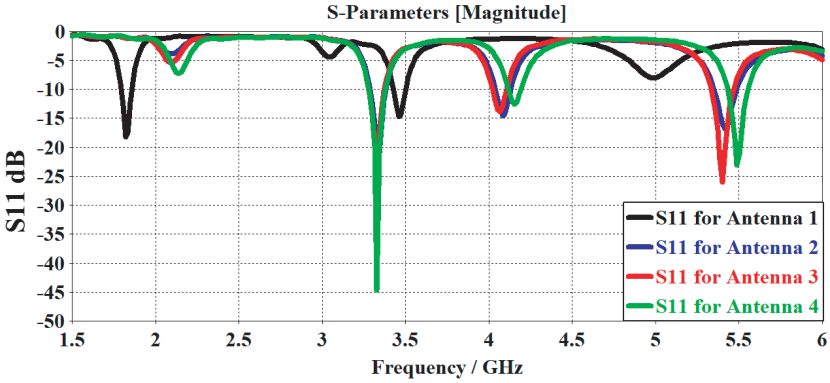

Figure 5. Simulated return loss (S_{11}) for the selected antennas.

The simulated radiation patterns for the above antennas were plotted at each resonant frequency. Due to space limitations, the 2D and 3D at a resonant frequency of around 3.3 GHz will be plotted for each antenna for comparison purposes. Figs. 7–10 show the 2D and 3D simulated radiation patterns for all antennas at different resonant frequencies. It can be clearly noted that the radiation patterns for all antennas are almost the same and exhibit nearly an omnidirectional pattern, which is preferable in this application. Table 1 compares the reflection and radiation characteristics of the designed antennas.

Table 1. Simulated characteristics of the designed antenna.

Antenna	Frequency (GHz)	S_{11} (dB)	Directivity (dBi)
Antenna 1	1.8195	−18.18	5.63
	3.458	−14.77	4.17
Antenna 2	3.3275	−21.66	5.53
	4.0815	−14.59	6.83
	5.4155	−16.78	4.45
Antenna 3	3.3275	−23.72	5.57
	4.067	−13.86	6.04
	5.401	−26.06	4.7
Antenna 4	3.3275	−44.68	5.5
	4.154	−12.57	4.42
	5.488	−23.04	4.98

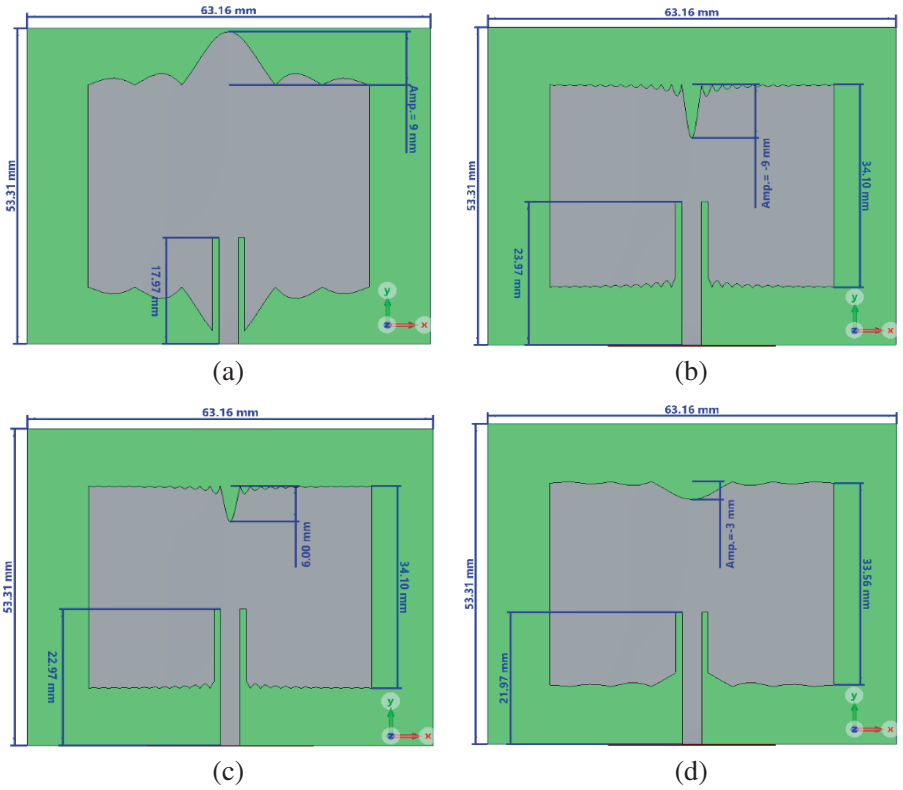

Figure 6. Structure and dimensions of the selected antennas: (a) Antenna 1 with $Amp. = 9\,\text{mm}$ and $m = 0.5$, (b) Antenna 2 with $Amp. = -9\,\text{mm}$ and $m = 2$, (c) Antenna 3 with $Amp. = -6\,\text{mm}$ and $m = 2$, (d) Antenna 4 with $Amp. = -3\,\text{mm}$ and $m = 0.5$.

4. EXPERIMENTAL RESULTS

The selected four antennas were manufactured as printed circuit board (PCB) on an FR-4 substrate as shown in Fig. 11. The reflection and radiation characteristics of the fabricated antennas were tested in

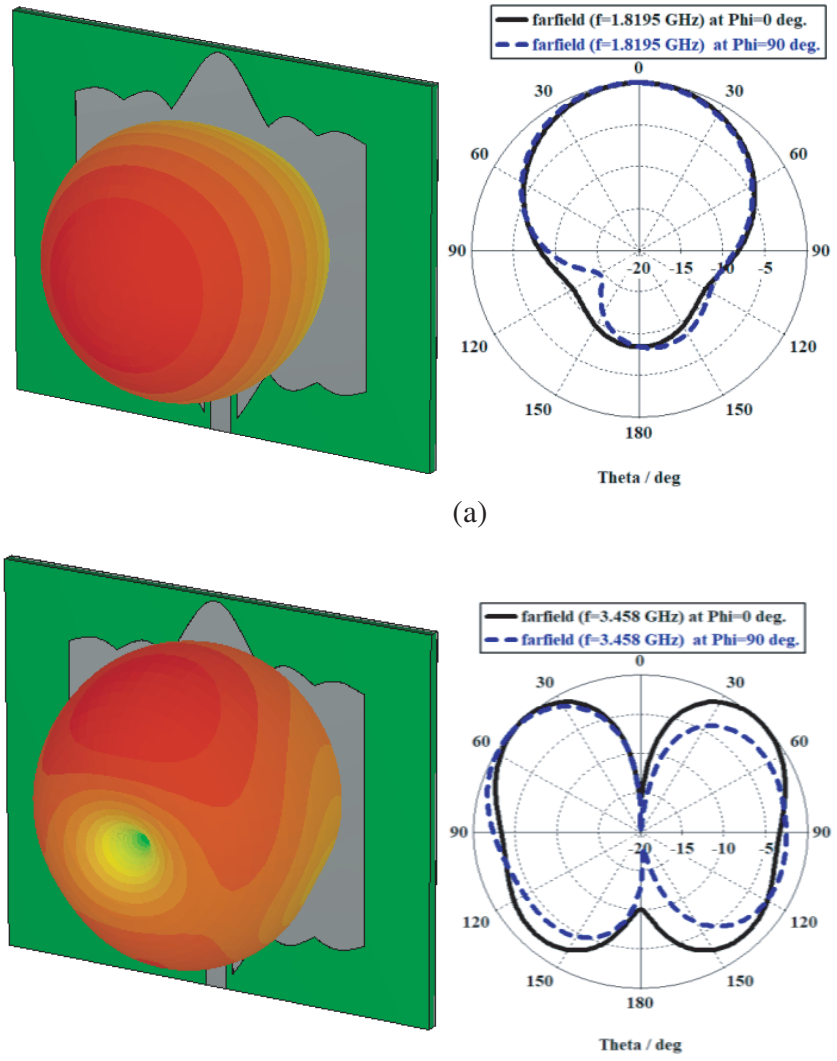

Figure 7. Simulated radiation pattern of Antenna 1 at different frequencies: (a) 1.81 GHz and (b) 3.45 GHz.

the lab within the frequency range 1.5–6 GHz. Fig. 12 illustrates the experimental setup used to test the performance of the antennas. An absorbing anechoic material is utilized to perform the measurement procedure with minimizing the reflections from the surrounding objects. Fig. 13 shows the measured return loss compared with the simulated ones. The results show that there is an excellent agreement between the experimental and simulated results at almost all frequency bands, which validate our simulation process.

It can be seen from Fig. 13 that the manufactured antennas exhibit multiband operations and resonate at different frequencies within the sub-6 GHz band mainly around 2 GHz, 3.3 GHz, 4 GHz, and 5.5 GHz. For getting accurate measured data, two identical versions of each antenna of the four antennas were fabricated for the sake of radiation pattern measurements.

RF source and spectrum analyzer were utilized to plot the measured radiation pattern in the lab with the aid of absorbing material to mimic anechoic environment and to eliminate reflections during the measurement process as shown in Fig. 12. Fig. 14 compares the simulated and measured radiation patterns.

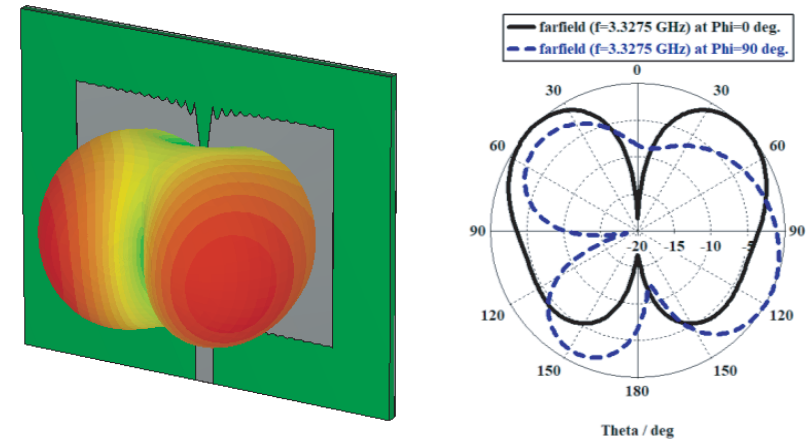

(a)

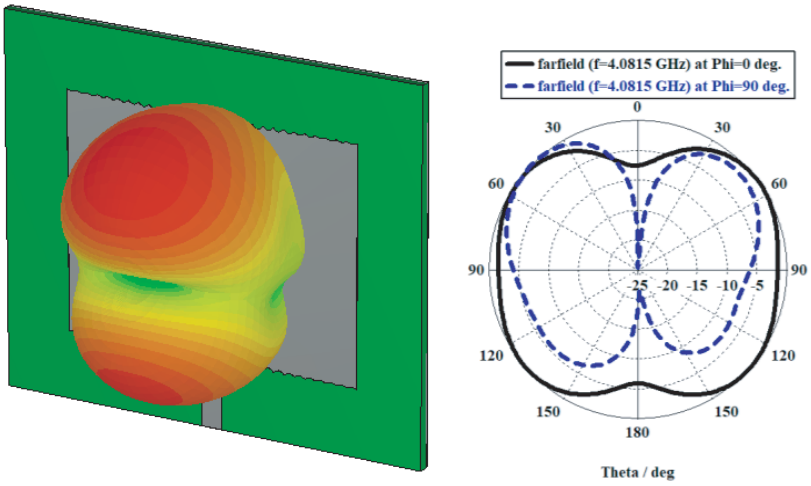

(b)

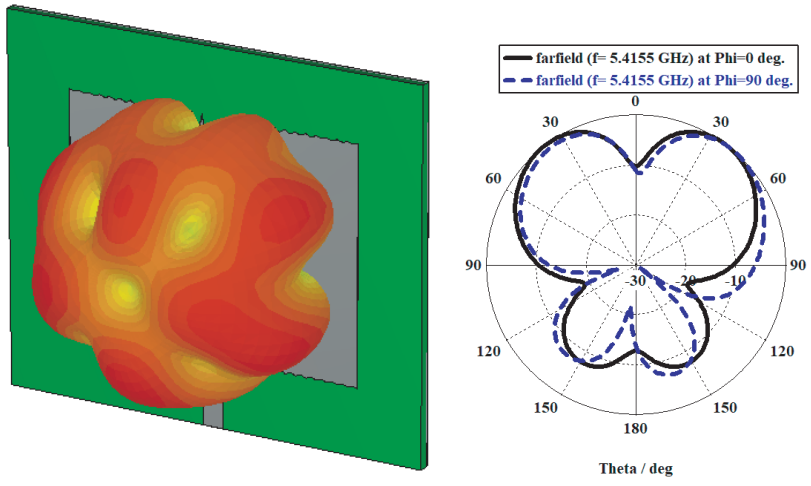

(c)

Figure 8. Simulated radiation pattern of Antenna 2 at different frequencies: (a) 3.32 GHz and (b) 4.08 GHz and (c) 5.41 GHz.

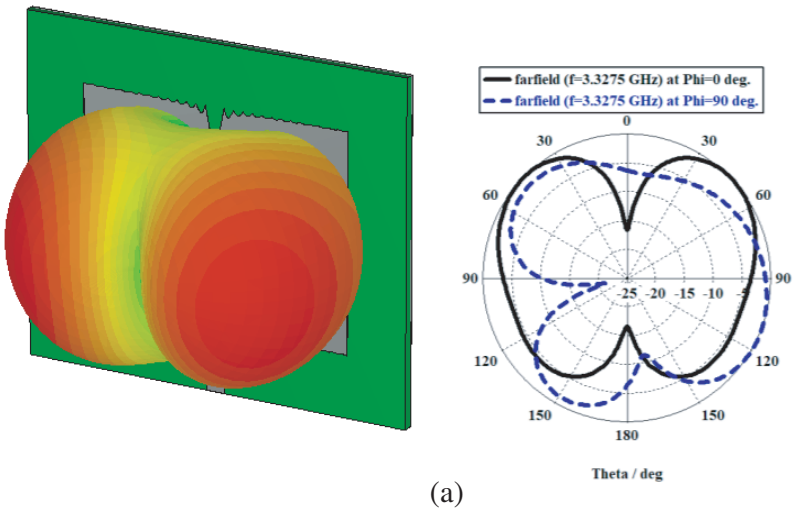

(a)

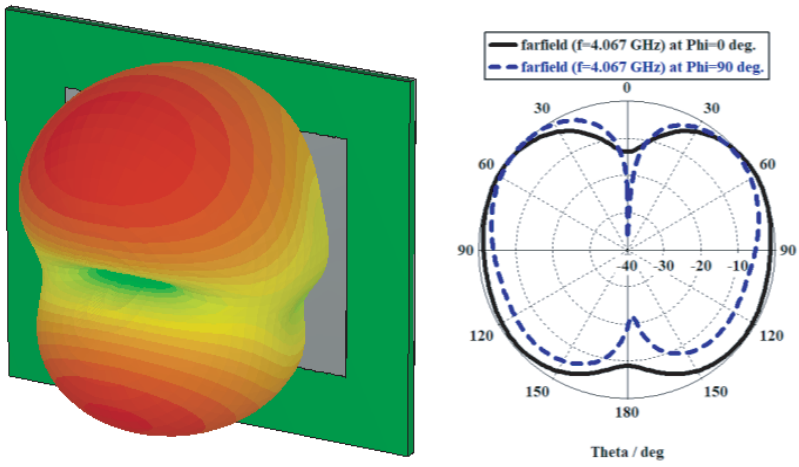

(b)

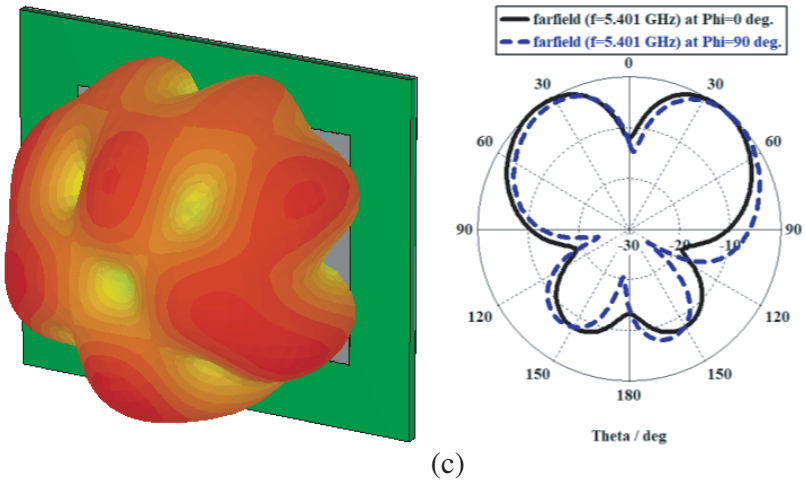

(c)

Figure 9. Simulated radiation pattern of Antenna 3 at different frequencies: (a) 3.32 GHz and (b) 4.06 GHz and (c) 5.40 GHz.

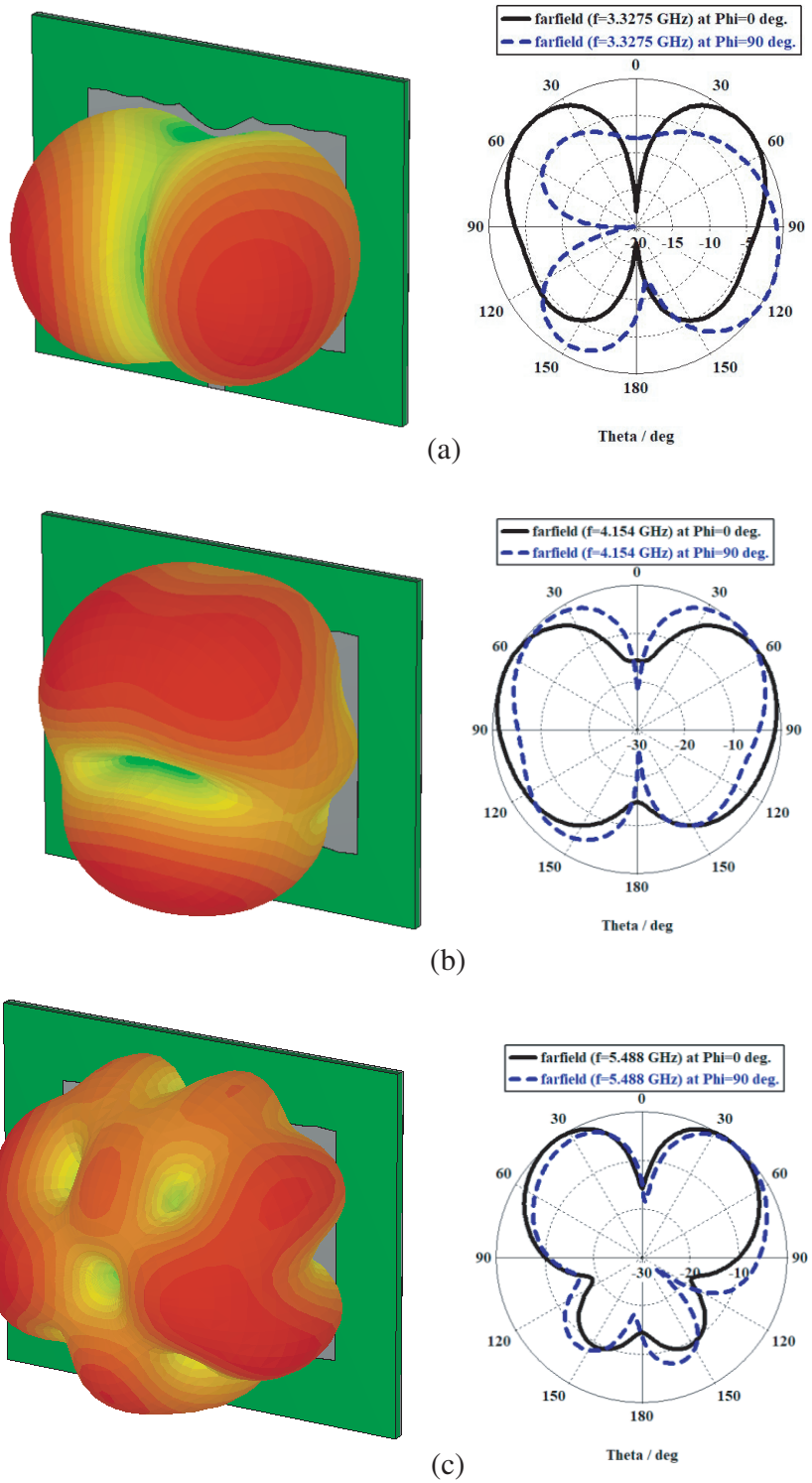

Figure 10. Simulated radiation pattern of Antenna 4 at different frequencies: (a) 3.32 GHz and (b) 4.15 GHz and (c) 5.48 GHz.

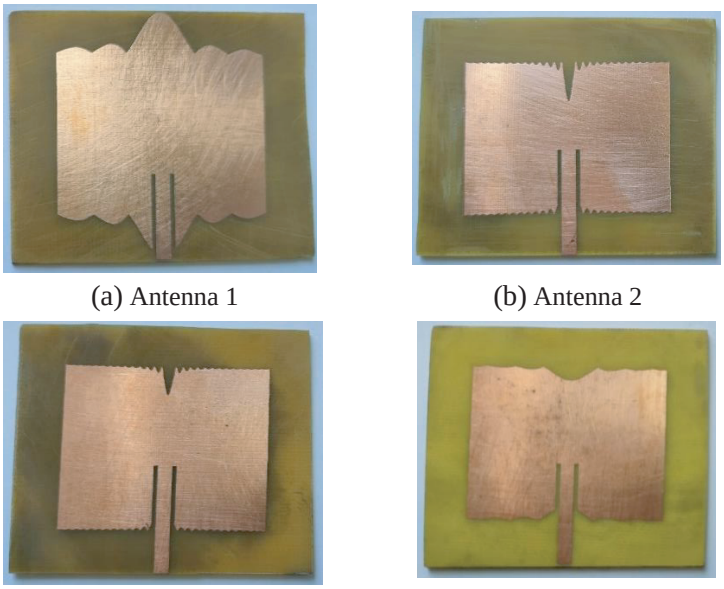

(a) Antenna 1 (b) Antenna 2

(c) Antenna 3 (d) Antenna 4

Figure 11. Photograph of the fabricated antennas.

Figure 12. Experimental setup showing the transmitting and receiving antennas.

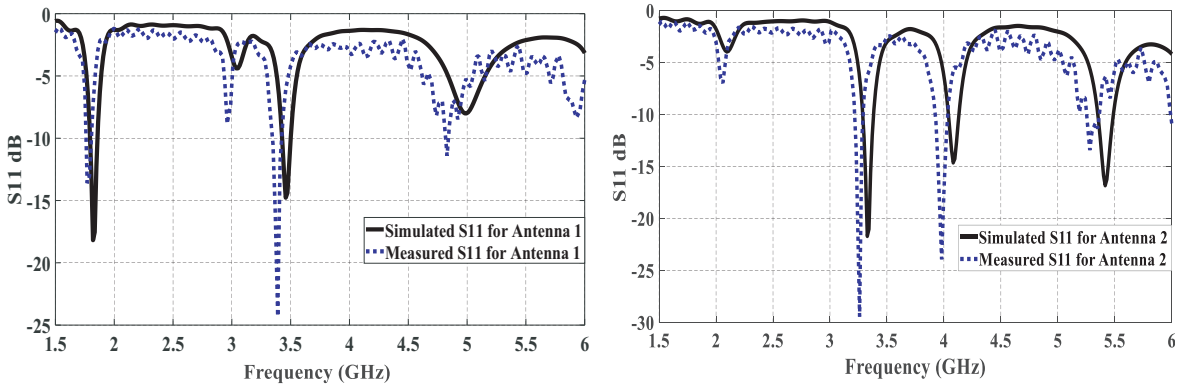

(a) Antenna 1 (b) Antenna 2

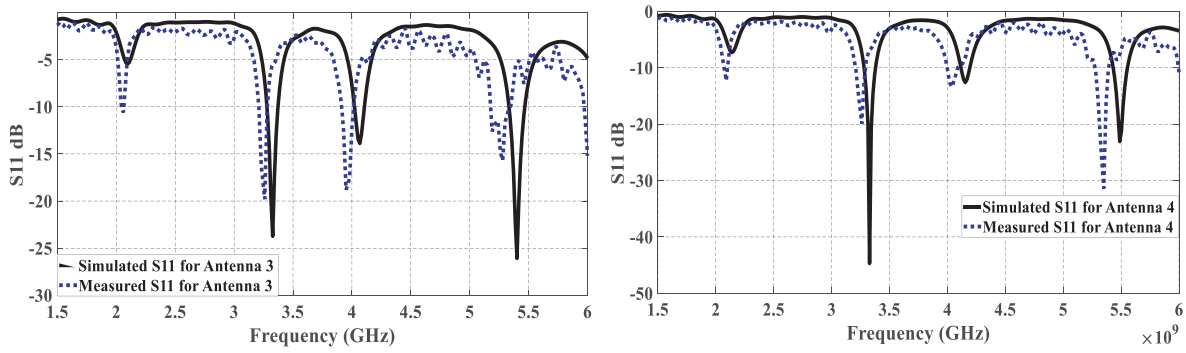

(c) Antenna 3 (d) Antenna 4

Figure 13. Simulated and measured S_{11} for proposed antennas.

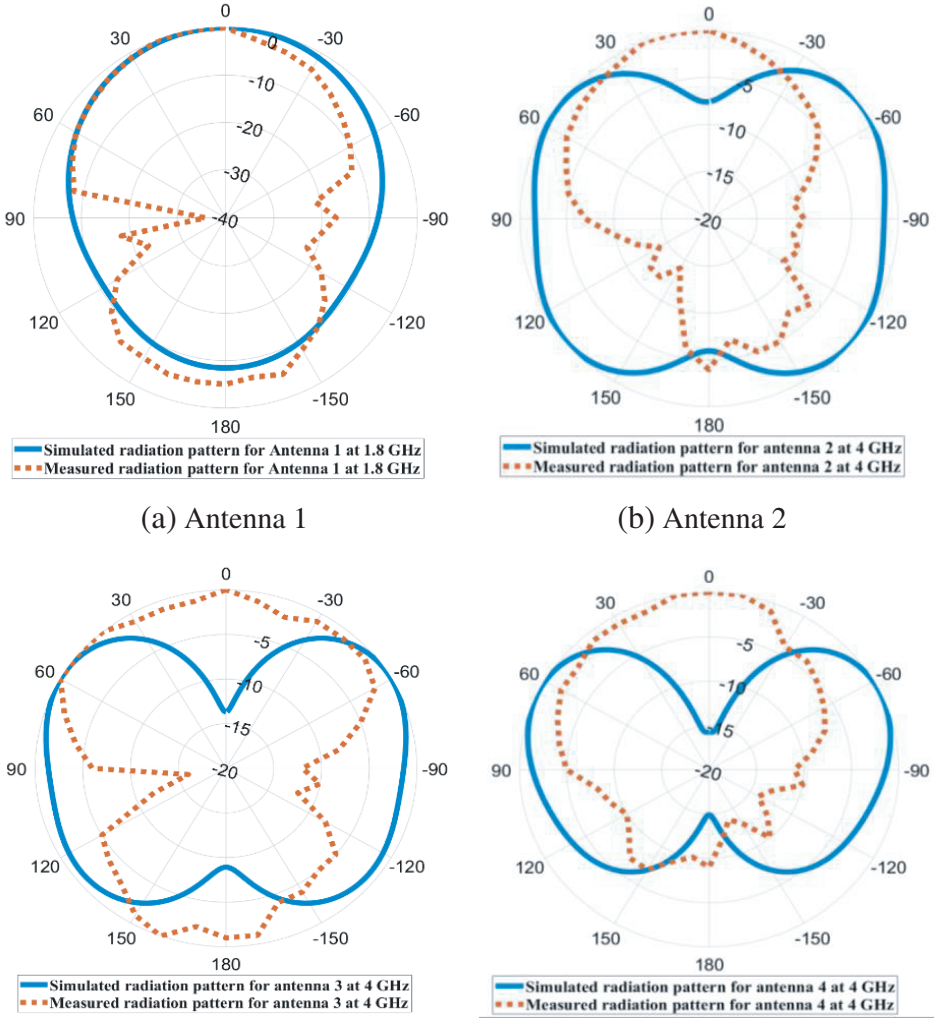

(a) Antenna 1 (b) Antenna 2

(c) Antenna 3 (d) Antenna 4

Figure 14. Simulated and measured 2D radiation pattern for the proposed sinc patch antennas measured at $\phi = 0$: (a) Antenna 1 at 1.8 GHz; (b) Antenna 2 at 4 GHz; (c) Antenna 3 at 4 GHz; and (d) Antenna 4 at 4 GHz.

5. CONCLUSION

In this paper, sinc function was utilized to control the performance of a rectangular patch antenna. The sinc function was integrated at the edges of the patch antenna to decrease or increase the length of the rectangular patch antenna. The impact of the sinc function parameters such as the amplitude and the frequency on the performance of the antennas was studied. The designed rectangular patch antennas with sinc-shaped edges antennas were validated by numerical simulations using CST Studio Suite. The return loss and 2D and 3D radiation patterns of the patch antennas were plotted. The results showed that there was a direct impact of the sinc function parameters on the resonant frequency of the antenna. It is found that the resonant frequency can be smoothly reduced by using positive sinc function, whereas it can be increased by employing negative sinc function. Four different antennas were selected out of the 35 simulated cases to be adopted for 5G application in this work. These antennas were also manufactured, and their characteristics were measured experimentally. The measured results agreed well with the simulated ones. Based on the achieved results of this paper, it is believed that the proposed approach of utilizing sinc function in the geometry of the antenna gives the designer an opportunity to tune the resonant frequency of the antenna freely and smoothly by changing the amplitude ($Amp.$) and frequency argument (m) of the incorporated sinc function.

REFERENCES

1. Patel, D. H. and G. D. Makwana, "A comprehensive review on multi-band microstrip patch antenna comprising 5G wireless communication," *International Journal of Computing and Digital System*, 941–953, 2021.
2. Hussain, W., M. I. Khattak, M. A. Khattak, and M. Anab, "Multiband microstrip patch antenna for 5g wireless communication," *International Journal of Engineering Works*, Vol. 1, No. 01, 15–21, 2020.
3. Milias, C., R. B. Andersen, P. I. Lazaridis, Z. D. Zaharis, B. Muhammad, J. T. B. Kristensen, A. Mihovska, and D. D. S. Hermansen, "Metamaterial-inspired antennas: A review of the state of the art and future design challenges," *IEEE Access*, Vol. 9, 89846–89865, 2021.
4. Wang, Z., Y. Ning, and Y. Dong, "Hybrid metamaterial-TL-based, low-profile, dual-polarized omnidirectional antenna for 5G indoor application," *IEEE Transactions on Antennas and Propagation*, Vol. 70, No. 4, 2561–2570, 2021.
5. Reis, J. R., M. Vala, T. E. Oliveira, T. R. Fernandes, and R. F. S. Caldeirinha, "Metamaterial-inspired flat beamsteering antenna for 5G base stations at 3.6 GHz," *Sensors*, Vol. 21, No. 23, 8116, 2021.
6. Murthy, N., "Improved isolation metamaterial inspired mm-Wave MIMO dielectric resonator antenna for 5G application," *Progress In Electromagnetics Research C*, Vol. 100, 247–261, 2020.
7. R. Saleem, M. B., H. T. Chattha, S. Ur Rehman, A. Mushtaq, and M. F. Shafique, "An FSS based multiband MIMO system incorporating 3D antennas for WLAN/WiMAX/5G cellular and 5G Wi-Fi applications," *IEEE Access*, Vol. 7, 144732–144740, 2019.
8. Nakmouche, M. F., A. M. Allam, D. E. Fawzy, and D.-B. Lin, "Development of a high gain FSS reflector backed monopole antenna using machine learning for 5G applications," *Progress In Electromagnetics Research M*, Vol. 105, 183–194, 2021.
9. Kumar, A., A. De, and R. K. Jain, "Gain enhancement using modified circular loop FSS loaded with slot antenna for sub-6 GHz 5G application," *Progress In Electromagnetics Research Letters*, Vol. 98, 41–48, 2021.
10. Ramahatla, K., M. Mosalaosi, A. Yahya, and B. Basutli, "Multiband reconfigurable antennas for 5G wireless and CubeSat applications: A review," *IEEE Access*, Vol. 10, 40910–40931, 2022.
11. Mukherjee, K., S. Mukhopadhyay, and S. Roy, "Design of wideband planar antenna with inverted I-shaped tuning stubs for application in 5G, satellite communication, and Internet of Things," *International Journal of Communication Systems*, Vol. 35, No. 11, e5191, 2022.

12. Alhamad, R., E. Almajali, and S. Mahmoud, "Electrical reconfigurability in modern 4g, 4g/5g and 5g antennas: A critical review of polarization and frequency reconfigurable designs," *IEEE Access*, Vol. 11, 29215–29233, 2023.
13. Asif, S. M., M. R. Anbiyaei, K. L. Ford, T. O'Farrell, and R. J. Langley, "Low-profile independently-and concurrently-tunable quad-band antenna for single chain sub-6 GHz 5G new radio applications," *IEEE Access*, Vol. 7, 183770–183782, 2019.
14. Sabaawi, A. M. A., K. S. Muttair, O. A. Al-Ani, and Q. H. Sultan, "Dual-band MIMO antenna with defected ground structure for sub-6 GHz 5G applications," *Progress In Electromagnetics Research C*, Vol. 122, 57–66, 2022.
15. Senger, S. and P. K.Malik, "A comprehensive survey of massive-MIMO based on 5G antennas," *International Journal of RF and Microwave Computer-Aided Engineering*, Vol. 32, No. 12, e23496, 2022.
16. Pant, M. and L. Malviya, "Design, developments, and applications of 5G antennas: A review," *International Journal of Microwave and Wireless Technologies*, 1–27, 2022.
17. Jiang, W., Y. Cui, B. Liu, W. Hu, and Y. Xi, "A dual-band MIMO antenna with enhanced isolation for 5G smartphone applications," *IEEE Access*, Vol. 7, 112554–112563, 2019.
18. Sabaawi, A. M. A., Q. H. Sultan, and T. A. Najm, "Design and implementation of multi-band fractal slot antennas for energy harvesting applications," *Periodica Polytechnica Electrical Engineering and Computer Science*, Vol. 66, No. 3, 253–264, 2022.